In Vivo Monitoring of Sevoflurane-induced Adverse Effects in Neonatal Nonhuman Primates Using Small-animal Positron Emission Tomography

Xuan Zhang, M.D., Ph.D., Shuliang Liu, M.D., Ph.D., Glenn D. Newport, B.S., Merle G. Paule, Ph.D., Ralph Callicott, D.V.M., Ph.D., James Thompson, B.S., Fang Liu, M.D., Ph.D., Tucker A. Patterson, Ph.D., Marc S. Berridge, Ph.D., Scott M. Apana, B.S., Christina C. Brown, B.S., Mackean P. Maisha, M.S., Joseph P. Hanig, Ph.D., William Slikker, Jr., Ph.D., Cheng Wang, M.D., Ph.D.

ABSTRACT

Background: Animals exposed to sevoflurane during development sustain neuronal cell death in their developing brains. *In vivo* micro-positron emission tomography (PET)/computed tomography imaging has been utilized as a minimally invasive method to detect anesthetic-induced neuronal adverse effects in animal studies.

Methods: Neonatal rhesus monkeys (postnatal day 5 or 6, 3 to 6 per group) were exposed for 8 h to 2.5% sevoflurane with or without acetyl-L-carnitine (ALC). Control monkeys were exposed to room air with or without ALC. Physiologic status was monitored throughout exposures. Depth of anesthesia was monitored using quantitative electroencephalography. After the exposure, microPET/computed tomography scans using ^{18}F-labeled fluoroethoxybenzyl-*N*-(4-phenoxypyridin-3-yl) acetamide (FEPPA) were performed repeatedly on day 1, 1 and 3 weeks, and 2 and 6 months after exposure.

Results: Critical physiologic metrics in neonatal monkeys remained within the normal range during anesthetic exposures. The uptake of [^{18}F]-FEPPA in the frontal and temporal lobes was increased significantly 1 day or 1 week after exposure, respectively. Analyses of microPET images recorded 1 day after exposure showed that sevoflurane exposure increased [^{18}F]-FEPPA uptake in the frontal lobe from 0.927 ± 0.04 to 1.146 ± 0.04, and in the temporal lobe from 0.859 ± 0.05 to 1.046 ± 0.04 (mean ± SE, $P < 0.05$). Coadministration of ALC effectively blocked the increase in FEPPA uptake. Sevoflurane-induced adverse effects were confirmed by histopathologic evidence as well.

Conclusions: Sevoflurane-induced general anesthesia during development increases glial activation, which may serve as a surrogate for neurotoxicity in the nonhuman primate brain. ALC is a potential protective agent against some of the adverse effects associated with such exposures. **(Anesthesiology 2016; 125:133-46)**

CLINICALLY used general anesthetics typically exert their action by the activation of inhibitory central nervous system (CNS) receptors, such as γ-aminobutyric acid (GABA) receptors, and/or the blockade of CNS excitatory receptors, such as *N*-methyl-D-aspartate (NMDA) receptors.[1–4] Many animal studies have shown that the developing brain is vulnerable to NMDA antagonists and/or GABA agonists: exposure to anesthetics during the period of rapid neuronal growth and synaptogenesis can induce massive neuroapoptosis.[3,5–7] These effects of general anesthetics are associated with subsequent, long-term behavioral deficits in both rats[6] and nonhuman primates.[8] Recently, several retrospective epidemiologic studies have indicated a relationship between general anesthesia in childhood and subsequent development of cognitive abnormalities and learning deficits in adolescence.[9–13] Therefore, it is necessary to study both the acute and long-term effects of early exposure to anesthetics on the developing CNS.

Sevoflurane is a commonly used inhalational anesthetic and has been frequently administered to pediatric patients during general anesthesia and sedation.[14–16] Sevoflurane is believed to activate glycine and GABA receptors type A and

What We Already Know about This Topic

- A wide variety of anesthetics induce neuronal apoptosis in the developing brain. Short of histopathologic analysis, our ability to identify neuronal injury *in vivo*, both spatially and temporally, is limited.
- The levels of peripheral benzodiazepine receptors, which are present in glia, increase in regions of neuronal injury. Importantly, ^{18}F-labeled fluoroethoxybenzyl-*N*-(4-phenoxypyridin-3-yl) acetamide can be used as a radioligand to image these receptors in the brain.
- Positron emission tomography was utilized to assess peripheral benzodiazepine receptor in the nonhuman primates exposed to sevoflurane. The effect of acetyl-L-carnitine was also investigated.

What This Article Tells Us That Is New

- Sevoflurane exposure increased glial activation, a surrogate for neurotoxicity, as indicated by increased uptake of ^{18}F-labeled fluoroethoxybenzyl-*N*-(4-phenoxypyridin-3-yl) acetamide in the frontal and temporal lobes.
- Acetyl-L-carnitine mitigated the adverse effects of sevoflurane.
- Peripheral benzodiazepine receptor can serve as biomarkers of anesthetic neurotoxicity; as such, the extent of anesthetic-induced injury can be evaluated spatially, noninvasively, and over longer periods of time *in vivo*.

Corresponding article on page 22. James C. Eisenach, M.D., served as Editor-in-Chief for this article. Dr. Zhang and Liu are co-first authors.

 Anesthesiology 2016; 125:133-46

<zdoi;10.1097/ALN.0000000000001154>

inhibit NMDA receptors.[17–20] In a neonatal rat model, a single episode of sevoflurane-induced general anesthesia (2 to 2.5% for 4 to 6 h) leads to widespread neuronal apoptosis in several brain regions and causes long-term behavioral impairments and memory dysfunction.[4,15,21–23] Repeated treatments with sevoflurane during gestation in the rat induced neuronal apoptosis in the brains of offspring.[24] In the mouse, exposure to sevoflurane on postnatal day (PND) 7 induced neuroapoptosis in the hippocampal region.[3,20,23,25–28] L-Carnitine (LC) has been shown to attenuate brain injury associated with mitochondrial dysfunction[29,30] and has been reported to provide neuroprotective benefits in a variety of neurodegenerative and aging situations.[31–35] In the current study, acetyl-L-carnitine (ALC) was utilized to evaluate its protective ability against adverse reactions associated with exposure to sevoflurane.

Positron emission tomography (PET) is a leading molecular imaging approach that provides quantitative information about biologic, biochemical, pathologic, and pharmacologic processes in living tissue and organs.[36–38] We have developed a microPET protocol to investigate possible neurotoxic effects associated with developmental exposures to sevoflurane *in vivo* using imaging approaches.[7,39–43]

In the CNS, translocator proteins (TSPOs, 18 KDa), previously known as peripheral benzodiazepine receptors, are primarily located in glial cells, and their levels are believed to increase in areas of neuronal injury after exposure to neurotoxicants.[44,45] Therefore, they are widely recognized as important targets for PET imaging.[45–47] In this study, ^{18}F-labeled fluoroethoxybenzyl-*N*-(4-phenoxypyridin-3-yl) acetamide ([^{18}F]-FEPPA) was utilized as a radiolabeled ligand for TSPOs/peripheral benzodiazepine receptors in the CNS of neonatal monkeys.

Nonhuman primate models are thought to be more relevant than rodent models because of their similarities to human beings in regard to the length of pregnancy, brain neuroanatomical organization, and pharmacodynamics after the administration of anesthetics, and we have used these models in previous studies.[41,48–50] In the current study, noninvasive monitoring of physiologic parameters in neonatal monkeys was utilized to evaluate whether homeostasis in the exposed animals was within the normal range during anesthesia.

Materials and Methods

Animals

All animal procedures were approved by the National Center for Toxicological Research (NCTR) Institutional Animal Care and Use Committee (Jefferson, Arkansas) and conducted in accordance with the Public Health Service Policy on Humane Care and Use of Laboratory Animals.

All nonhuman primates were born and housed at the NCTR nonhuman primate research facility. Animal procedures were designed to minimize the number of animals required and any pain or distress associated with the experimental procedures. Neonatal rhesus monkeys (*Macaca mulatta*) were obtained from the NCTR breeding colony as previously described.[50] Briefly, breeder monkeys were housed in separate cages under a 12:12-h light/dark cycle, provided with water *ad lib* and fed high-protein jumbo monkey diet supplemented routinely with fresh fruit. All births occurred *via* natural delivery, and the day of birth was designated as PND 0. Neonatal monkeys stayed with their mothers except during anesthetic exposure or control sequestrations, until they were weaned at 6 months of age.

A total of 18 neonatal (PND 5 or 6, 460 to 500 g) rhesus monkeys were utilized. Ten male and 8 female monkeys were randomly assigned to experimental groups: control (n = 4, 3 male and 1 female), control + ALC (n = 4, 2 male and 2 female), sevoflurane alone (n = 4, 1 male and 3 female), and sevoflurane + ALC (n = 6, 4 male and 2 female). About 30 min before the initiation of anesthesia or sequestration (controls), the neonates were separated from their mothers and hand-carried to a procedure room. Control animals were maintained in an incubator with the temperature set at 32°C, with no water or food, and were not sedated for physiologic measurements or blood sample collections. Animals in the anesthetic exposure groups were exposed to 2.5% sevoflurane in oxygen for 8 h.

To examine the severity and the nature of sevoflurane anesthetic–induced neuronal damage, an additional six monkey infants (exposed on either PND 5 or 6) were randomly assigned to a sevoflurane-alone group (n = 3) and a control, room air exposure group (n = 3).

Experimental Procedures

Neonatal rhesus monkeys were treated following procedures described previously.[39] Briefly, animals were exposed on PND 5 or 6 to sevoflurane within a clear anesthesia induction chamber (18 × 9 × 8 in; E-Z Anesthesia®, USA). Sevoflurane (Webster Veterinary Supply, USA) along with oxygen (nexAir, USA) was delivered from a sevoflurane-specific vaporizer (Tec 7, Baxter, USA) at a concentration of 2.5% (v/v) into the chamber at a rate of about 0.5 to 1.0 l/min. The induction chamber was warmed from the bottom by a heat therapy pump (T/PUMP®, Gaymar Industries, USA). For controls, room air was used in place of the sevoflurane. A relief valve on the anesthesia chamber allowed the escape of gases to avoid accumulation of carbon dioxide, and waste anesthetic gas was scavenged using an attached canister containing activated charcoal. For animals receiving ALC (Sigma-Aldrich, USA), it was administered intraperitoneally at doses of 100 mg/kg in a saline vehicle,

Submitted for publication June 24, 2015. Accepted for publication March 23, 2016. From the Divisions of Neurotoxicology (X.Z., S.L., G.D.N., M.G.P., F.L., T.A.P., C.W.) and Bioinformatics and Biostatistics (M.P.M.) and Priority One Services (R.C., J.T.), National Center for Toxicological Research, U.S. Food and Drug Administration, Jefferson, Arkansas; 3D Imaging, LLC, Little Rock, Arkansas (M.S.B., S.M.A., C.C.B.); and Center for Drug Evaluation and Research/U.S. Food and Drug Administration, Silver Spring, Maryland (J.P.H., W.S.).

1 h before and 4 h after the start of exposure to room air or the anesthetics. Anesthetized monkeys were maintained in a laterally recumbent position.

During exposures, a stomach tube (5 ml) was used to administer 5% dextrose and 0.45% sodium chloride (Baxter) every 2 h to both treated and control monkeys to maintain blood glucose levels. All subjects were administered two doses of glycopyrrolate (American Regent, USA; 0.01 mg/kg, intramuscularly) at 0 and 6 h during exposure to reduce airway secretions. Animals were monitored in the incubator until complete recovery and then returned to their mothers (approximately 2 h after exposure). Control animals were kept in the infant incubator under room air for 8 h.

Monitoring of Physiologic Parameters

Physiologic parameters of all subjects were monitored following procedures previously described.[49,50] Briefly, noninvasive pulse oximetry (N-395 Pulse Oximeter, Nellcor, USA; MouseO_X Plus Vital Sign Monitor, Starr Life Sciences, USA), capnography (Tidal Wave Hand-held capnography, Respironics, USA), sphygmomanometry (Critikon Dinamap Vital Signs Monitor, GE Healthcare, USA), and a rectal temperature probe were used to verify the physiologic status of subjects during the exposures and sequestrations. Heart and respiration rates, arterial blood oxygen saturation levels, expired carbon dioxide concentrations, rectal temperatures, and systolic and diastolic blood pressures were recorded every 2 h in anesthetized and control animals. Venous blood (approximately 300 μl) was collected at 2-h intervals for measurement of plasma glucose concentrations, venous blood gases, pH values, and hematocrits (GEM® Premier 4000, Instrumentation Laboratory, USA). During microPET scans, the peripheral oxygen saturation, heart rate (HR), respiration rate, and rectal body temperature were recorded every 15 min.

Monitoring the Depth of Anesthesia Using Quantitative EEG

The depth of anesthesia was assessed by monitoring the alteration of cortical electrical activity using quantitative electroencephalogram (EEG) technology. A SEDLine system (Masimo Corp, USA) was utilized to monitor neonatal monkeys during exposure to sevoflurane, according to the operator's manual provided by the manufacturer.[51] Briefly, the four-channel EEG sensor comprising 6 pregelled electrodes was connected to the animal's head to collect analog EEG data. The analog EEG data were converted to digital data by the patient module connected to the sensor. Then the digital data were transferred to a computer and monitor, where they were processed, analyzed, and displayed. A patient state index (PSI), which is indicative of the level of consciousness/anesthesia, was generated using an algorithm developed on the basis of extensive EEG recordings.[52] The PSIs range from a scale of 0 to 100, where 100 represents the fully awake state. The optimal level of anesthesia was represented by PSIs within the range of 25 to 50. Real-time PSI data, including the associated .csv log files, were later transferred to external storage medium for statistical analysis and plotting. Background noise from muscular electrical activity and nonbrain electrical artifacts can interfere with the waveform of the EEG. Thus, the PSI values were generated only when the contributions from background nonbrain electrical activities were sufficiently low, as indicated by electromyographic data. The electromyographic data, a record of muscle activity, such as jaw clenching, ranged from a value of 0 to 100% and was plotted as a bar graph for review.

Radiotracer Preparation

[^{18}F]-FEPPA was prepared by 3D Imaging LLC (USA) according to the procedure of Wilson *et al.*[47] from the corresponding tosylate as described therein with minor modifications. [^{18}F]-FEPPA was produced in more than 98% purity at a specific activity at end of synthesis of 1.1 to 3.7 TBq (30 to 100 Ci)/μmol, as compared to the previously reported value of 11 to 37 GBq (0.3 to 1 Ci)/μmol.[53] Specific activity at the time of use was one tenth to two thirds of the end of synthesis value.

MicroPET

A commercial high-resolution small-animal PET scanner (Focus 220, Siemens Preclinical Solution, USA) was used to quantitatively record images of the monkey brain. The scanner has 96 lutetium oxyorthosilicate detectors and provides a transaxial resolution of approximately 1.35-mm full-width at half-maximum. Data were collected in a 128 × 128 × 95 matrix with a pixel width of 0.475 mm and a slice thickness of 0.815 mm.

Computed Tomography

Monkeys were also imaged in a newly developed mobile neurologic CereTom CT scanner (Neurologica Co., USA). The computed tomography (CT) gantry of the CereTom scanner moves while the subject remains externally supported and fixed in space, therefore allowing it to be physically connected to the microPET scanner. Exposure settings for each CT scan were 120 kVp, 5 mAs, and scan time = 120 s. Data were collected in a 512 × 512 matrix with a pixel width of 0.49 mm and a slice thickness and space of 2.5 mm.

MicroPET/CT Image Acquisition

The first microPET and CT scans of each monkey brain were taken on PND 6 or 7, the day after experimental exposures on PND 5 or 6. Follow-up microPET/CT scans occurred at approximately 1 week (on PND 14), 3 weeks (on PND 30), and 2 and 6 months of age. For collection of the microPET/CT images, animals were positioned on a modified external bed controlled by the microPET manager. Instead of the standard microPET bed, this modified bed allowed for enough travel to move animals through the

microPET and CT fields of view (over an axial range of greater than 50 cm). Throughout the microPET/CT imaging sessions (120 to 130 min), monkeys were anesthetized with 1.2 to 1.5% isoflurane gas alone delivered through a custom facemask, and an electronic heating pad was used to maintain body temperature at approximately 37°C. A transmission scan (10 min) with a rotating ^{57}Co point source was performed using software supplied by the scanner manufacturer. For each imaging session, [^{18}F]-FEPPA (56 MBq) was injected into the lateral saphenous vein of each animal (anesthetized). Immediately after the injection, a set of serial microPET images was recorded to assess the influx and accumulation of the tracer over the next 2 h (24 frames, 5 min each). Immediately after microPET imaging, microCT brain images of the animal were obtained in about 2 min for the purpose of coregistering anatomical (CT) with molecular (PET) data. Emission data were reconstructed as 3D volumes including scatter and attenuation correction using 3D reconstruction software (ASIPro, Concorde Microsystems, Inc., USA) installed in the CereTom CT controller unit. Once scanning was complete, animals were monitored in an incubator within a shielded isolation area until complete recovery and then returned to their mothers.

Imaging Data Analysis

Medical image analysis software (ASIPro, Concorde Microsystems, Inc.) was used for the anatomical/molecular data coregistration and analyses. Regions of interest (ROIs) were outlined and measured using tools provided by ASIPro. Radioactivity in different brain areas was also quantified using this software. All images were displayed using the same color scale. Tracer accumulations in the ROIs in the left thalamus, left frontal, and left temporal cortex were converted to standard uptake values (SUVs).

Fluoro-Jade C Staining

To examine the severity and the nature of sevoflurane anesthetic–induced neuronal damage, an additional six monkey infants (exposed on either PND 5 or 6) were randomly assigned to a sevoflurane-alone group (n = 3) and a control, room air exposure group (n = 3). The frontal lobe/cortex was chosen for pathologic analysis. Coronal sections (40 μm) of the frontal cortex were sectioned with a cryostat for Fluoro-Jade C (Histo-Chem, Inc., USA) staining as previously described.[54] Briefly, before staining, sections were mounted onto polylysinized slides. The mounted sections were bathed in a solution of 1% sodium hydroxide in 80% ethanol for 5 min and washed in 70% ethanol and distilled water for 2 min, respectively, followed by an incubation in 0.06% potassium permanganate solution for 10 min and another incubation in a 0.0001% solution of Fluoro-Jade C (Histo-Chem, Inc.) dissolved in 0.1% acetic acid vehicle for 10 min. A stock solution of 0.01% Fluoro-Jade C was prepared before being diluted to the 0.0001% working solution. The slides were rinsed through three changes of distilled water for 1 min per change. The air-dried slides were cleaned in xylene, and a cover-slip was applied with DPX nonfluorescent mounting media (Sigma, USA).

Statistical Analysis

Radiotracer accumulation in the ROIs was converted to SUVs (SUVs = total radioactivity in ROI × body weight of monkey/injection dose of [^{18}F]-FEPPA). All SUVs for the ROIs obtained from the microPET image were presented as mean ± SEM and compared between groups at a variety of time points using one-way ANOVA with Tukey *post hoc* analysis using SigmaPlot (Systat Software Inc., USA). A linear mixed model was used to evaluate the effect of treatment on physiologic parameters. A compound symmetry covariance structure in the context of repeated measures ANOVA was used to model covariance patterns of repeated measurements on the same animal assuming homogeneous variance/covariance. In the presence of any significant interactions, treatment comparisons were performed within each time point; otherwise, the mean comparisons were evaluated for each main effect. Planned treatment comparisons were performed between each sevoflurane-exposed group and the control group. The Dunnett test was performed in multiple pairwise comparisons between the fixed control group and the other treatment groups. The Bonferroni correction was used in the multiple pairwise tests on physiologic monitoring data sets acquired at multiple time points from the same set of animals. Student's *t* test was used for the PSI comparisons between the sevoflurane-exposed groups with or without ALC and the comparison of Fluoro-Jade C staining between control and sevoflurane-exposed monkeys. All statistical tests in the analyses are two sided unless otherwise stated. Throughout this article, statistical significance was assessed at the 5% nominal level ($\alpha = 0.05$). Multiplicity adjustments were performed to preserve the type I error rate at the specified nominal level.

Results

Critical Physiologic Measures Were within the Normal Range during 8-H Sevoflurane Exposures in the Neonatal Monkey

Throughout the 8-h exposures or sequestrations, vital signs, including HR, blood pressure, respiration rate, end-tidal carbon dioxide (ET_{CO_2}), rectal temperature, and blood oxygen saturation, were monitored closely. Analysis of venous blood every 2 h also demonstrated that there were no significant alterations in pH, glucose, hematocrit, carbon dioxide or oxygen partial pressures, or hemoglobin oxygenation throughout the exposures (table 1).

Respiration rate was moderately lower in the sevoflurane-exposed animals (57.4 ± 5.0) in comparison with the control animals (72.7 ± 5.8), without statistical significance ($P = 0.10$). Throughout the exposure, the differences in respiration rates between these two groups were not statistically significant ($P > 0.05$), with an exception at 4 h ($P = 0.011$).

Table 1. Physiologic Parameters and Blood Gas Values* for Sevoflurane-exposed and Control Animals

Group	Control	Control + ALC	Sevoflurane	Sevoflurane + ALC
Heart rate (beats/min)	225.0 ± 8.7	217.4 ± 8.4	165.0 ± 7.5†	157.8 ± 7.8†
Breath rate (beats/min)	72.7 ± 5.8	75.1 ± 5.8	57.4 ± 5.0	63.6 ± 5.3
Expired carbon dioxide (mmHg)	15.7 ± 2.0	16.6 ± 2.0	21.8 ± 1.7	21.9 ± 1.8
Rectal temperature (°F)	99.7 ± 0.5	99.4 ± 0.5	97.3 ± 0.5†	96.8 + 0.5†
Systolic blood pressure (mmHg)	119.3 ± 7.3	102.8 ± 7.3	125.7 ± 6.3	103.4 ± 6.8
Diastolic blood pressure (mmHg)	93.6 ± 7.5	72.7 ± 7.5	97.6 ± 6.5	75.1 ± 6.9
Mean arterial pressure (mmHg)	102.2 ± 7.3	82.8 ± 7.3	106.9 ± 6.3	84.5 ± 6.8
Pulse oxygen saturation (%)	96.7 ± 0.6	96.7 ± 0.6	97.7 ± 0.5	97.9 ± 0.5
Blood glucose (mg/dl)	58.7 ± 6.6	62.7 ± 6.4	55.4 ± 5.7	60.4 ± 6.0
Blood pH	7.19 ± 0.02	7.22 ± 0.02	7.27 ± 0.02	7.25 ± 0.02
Hematocrit (%)	47.8 ± 2.2	49.3 ± 2.1	51.7 ± 1.8	48.1 ± 1.8
Venous blood P_{CO_2} (mmHg)	53.9 ± 2.8	48.9 ± 2.7	57.0 ± 2.5	58.9 ± 2.5
Venous blood P_{O_2} (mmHg)	23. 9 ± 2.0	26.4 ± 2.0	24.5 ± 1.8	25.7 ± 1.9
Total hemoglobin (g/dl)	16.7 ± 0.8	17.3 ± 0.8	18.2 ± 0.6	16.7 ± 0.6
Venous blood oxyhemoglobin (%)	29.6 ± 5.4	41.4 ± 5.6	38.4 ± 4.1	34.2 ± 4.0
Venous blood hemoglobin (%)	68.3 ± 5.5	56.3 ± 5.8	59.6 ± 4.2	63.5 ± 4.1
Venous blood oxygen saturation (%)	30.3 ± 5.6	42.4 ± 5.8	39.2 ± 4.2	35.0 ± 4.1

*Statistically significant at $P < 0.05$ *vs*. the "control" group. †Mean ± SE.
ALC = acetyl-L-carnitine; P_{CO_2} = partial pressure (tension) of carbon dioxide.

Overall, the differences in ET_{CO_2} were not statistically significant ($P = 0.07$), except at 8 h when ET_{CO_2} was significantly higher in the anesthetized animals, 25.6 ± 2.3 *versus* 14.3 ± 2.6 in controls ($P = 0.005$). Importantly, arterial blood oxygen saturation, carbon dioxide and oxygen partial pressures, as well as venous oxyhemoglobin, deoxyhemoglobin, blood glucose, and pH, did not differ between the sevoflurane-exposed monkeys and controls. Taken together, these data demonstrate that neither compromised ventilation and respiratory acidosis nor hypoglycemia occurred in the sevoflurane-exposed animals. Volatile and other general anesthetics are well known to cause myocardial suppression. In the current study, the HR of sevoflurane-exposed neonatal monkeys was moderately reduced in comparison with that of control animals ($P = 0.022$); however, there were no significant effects on blood pressure ($P > 0.05$). The decrease in HR in the sevoflurane-exposed animals occurred as early as 2 h after the start of exposure ($P < 0.001$) and remained steady thereafter. Sevoflurane-induced changes of HR and respiration rate were consistent with previous studies related to ketamine.[49,50] The sevoflurane-exposed animals also experienced a slight yet significant ($P < 0.001$) drop in core body temperature. As five blood samples were taken during the 8 h of observation, the hematocrit in all groups declined slightly over time ($P < 0.05$). The coadministration of ALC alone did not have any significant effects on any of vital sign parameters described in the Monitoring of Physiologic Parameters in Materials and Methods ($P > 0.05$).

Depth of Anesthesia Was Not Altered by Coadministration of ALC

To evaluate the effects of coadministered ALC on the depth of anesthesia, quantitative EEG analysis was used to determine the level of brain activity during sevoflurane exposure. In all 15 sevoflurane-exposed subjects, the contributions of muscular electrical activity were found to be without consequence. The numerous PSIs recorded throughout the sevoflurane exposures were averaged within each subject for comparison of the effects between the sevoflurane-alone group and the sevoflurane plus ALC group. The mean PSI for the sevoflurane-alone group (32.7 ± 4.8) was no different from that for the sevoflurane plus ALC group (32.9 ± 4.8). The similar levels of the PSIs for the two groups are evidenced by representative samples from several subjects recorded 1, 4, and 7 h after the start of sevoflurane exposure (fig. 1). In addition to brain electrical activity, several physiologic parameters also served as traditional indicators of depth of anesthesia. Here, there were no significant differences between the sevoflurane-alone and sevoflurane plus ALC groups with respect to HR ($P = 0.829$), mean arterial pressure ($P = 0.113$), or ET_{CO_2} ($P = 0.981$) throughout the 8-h exposure.

Coregistration of MicroPET Images with CT Images for Anatomical Localization

Coronal CT images were obtained immediately after the microPET scans for the purpose of anatomical/molecular data coregistration. Figure 2 represents the microPET ([^{18}F]-FEPPA)/CT brain images from a sevoflurane-exposed monkey: the PET/CT images were fused using ASIPro software. By using the Fusion Tool in the ASIPro software, multiple data sets (anatomical and functional) can be loaded in the same general orientation and viewed using either linked or fused views. As shown in figure 2, the anatomical (CT) images are displayed in the top row and the functional (microPET) images in the bottom row. Once the images were loaded, the anatomical images were transposed onto the functional images and "fused" images were created, as

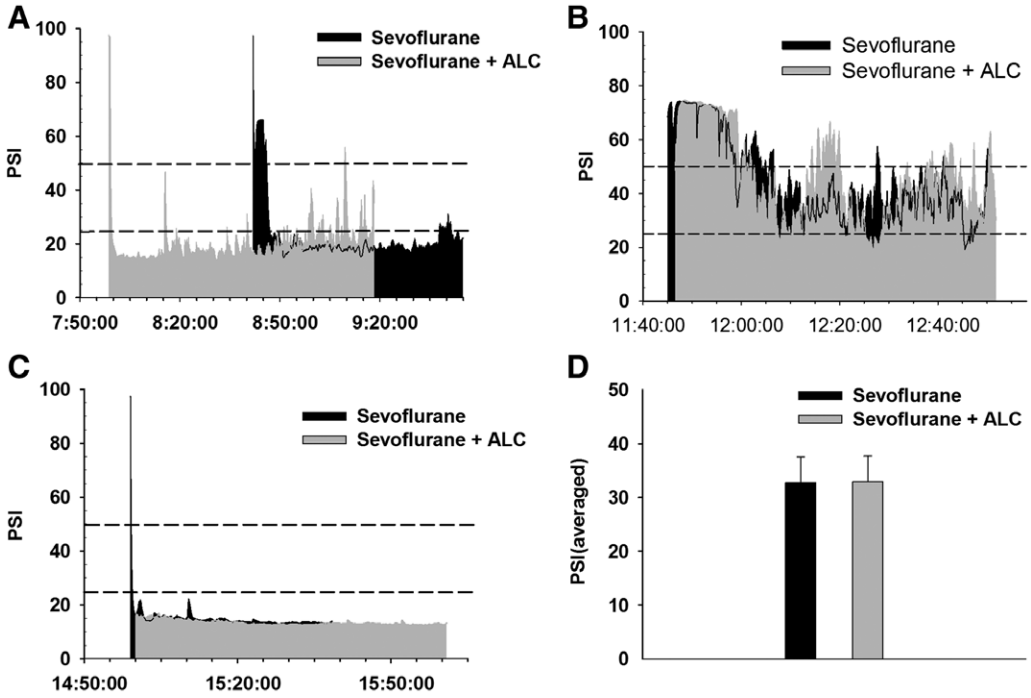

Fig. 1. The depth of anesthesia under 2.5% sevoflurane as measured by quantitative electroencephalography was not altered by the coadministration of acetyl-L-carnitine (ALC). The level of brain electric activities for those postnatal day 5/6 monkeys with (n = 8) or without (n = 7) coadministration of ALC was monitored throughout the sevoflurane exposure. The patient state index (PSI), a dimensionless index, generated in real time by analysis of the electroencephalogram, was used as a metric of the level of anesthesia. PSIs in the range from 25 to 50, as indicated by the *dashed lines*, correspond to an optimal level of anesthesia. Representative PSIs for animals from the sevoflurane-exposed and sevoflurane exposed with coadministration of ALC are shown at 1 (*A*), 4 (*B*), and 7 h (*C*) after the start of anesthesia. Comparisons of the mean PSIs for the two groups confirmed that there were no significant differences between them (*D*; $P = 0.97$, Student's *t* test).

seen in the middle row. Coupling microPET ([18F]-FEPPA) with CT, the imaging data indicate that sevoflurane-induced neural damage was located primarily in cortical brain levels including the frontal and temporal lobes, as well as in the thalamus.

Dynamic [18F]-FEPPA Uptake and Increased Neuronal Damage in the Frontal Cerebral Cortex

Eight hours of sevoflurane exposure produced significant increases in the accumulation of [18F]-FEPPA signals in neocortical areas, especially the frontal cortex (fig. 3), as evidenced by data collected from coronal scans obtained 1 day after sevoflurane exposure. All images were displayed using the same color scale shown in figure 3.

In addition, sevoflurane-induced neurotoxicity was assessed using Fluoro-Jade C staining. Fluoro-Jade C–stained neurons are characterized by high resolution and great contrast, and therefore, the degenerating neurons can be precisely localized.[54] The 8-h exposure to a clinically relevant concentration of sevoflurane (2.5%) produced extensive neuronal damage as indicated by increased Fluoro-Jade C-positive neuronal cells in the frontal cortex (fig. 4).

After the first microPET/CT scan was taken on PND 6 or 7, follow-up scans were obtained for each animal 7 days (PND 14), 21 days (PND 30), 2 months, and 6 months after sevoflurane exposure. For each microPET scan, images were obtained over 2 h after the injection of [18F]-FEPPA, and time activity curves from the frontal cortex (the most vulnerable brain area)[30,55] were obtained, as were those from the temporal lobe and thalamus. Tracer accumulations in the ROIs were converted to SUVs.

In the current study, the accumulation of [18F]-FEPPA was clearly increased in frontal cortical ROI in sevoflurane-exposed monkeys 1 day after exposure (fig. 5A). Coadministration of ALC effectively blocked this increase in retention of the [18F]-FEPPA signal induced by sevoflurane. There was no significant effect of ALC on SUVs when given alone.

On PND 14, approximately 7 days after the anesthetic exposure, SUVs in the frontal area were still significantly higher in the exposed animals than in the controls at most of the time points, demonstrating a prolonged increased uptake and retention of [18F]-FEPPA in treated subjects (fig. 5B). Compared with controls, there was no significant difference in SUVs detected in animals treated with sevoflurane plus ALC.

On PND 30, about 3 weeks after anesthetic exposure, the uptake of [18F]-FEPPA in the anesthetic-exposed monkeys remained higher than that seen in the controls at most time points, but there were no statistically significant findings at any specific time point (fig. 5C) at that time. This is likely due to the small number (n) used to derive these data. At

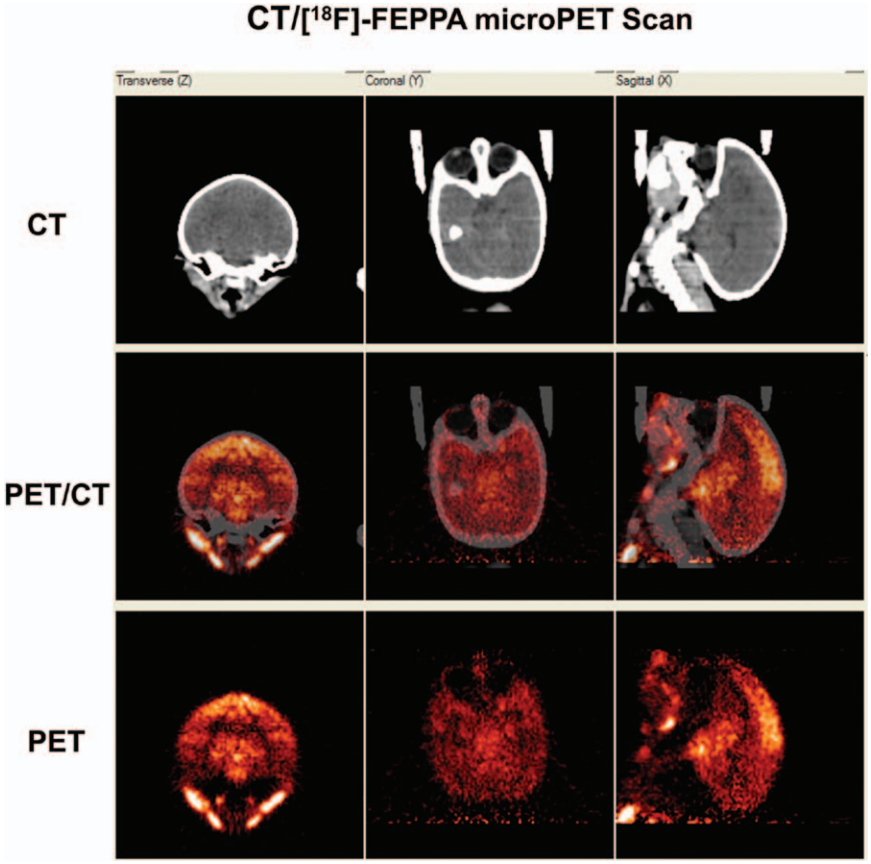

Fig. 2. Micro-positron emission tomography (microPET)/computed tomography (CT) brain images from a sevoflurane-exposed monkey injected with 56 MBq of ^{18}F-labeled fluoroethoxybenzyl-*N*-(4-phenoxypyridin-3-yl) acetamide ([^{18}F]-FEPPA). The PET/CT images were fused using ASIPro software (Concorde Microsystems, Inc., USA). *Top*: CT images; *bottom*: microPET images; *middle*: fused PET/CT images.

2 and 6 months of age, the uptake of [^{18}F]-FEPPA in the anesthetic-exposed monkeys returned to similar levels to that observed in controls at most time points (no significant differences were observed at any time; data not shown).

[^{18}F]-FEPPA Uptake in the Temporal Cerebral Cortex and Thalamus

On PND 6/7 (1 day after exposure), the accumulation of [^{18}F]-FEPPA in the ROIs in the temporal area and thalamus was also quantitated. At this time, the accumulation of [^{18}F]-FEPPA was increased in the temporal cortical lobe (fig. 6) and thalamus (fig. 7) in sevoflurane-exposed brains over virtually all time points. However, these differences were only statistically significant in the temporal lobe for a few specific time points (fig. 6A). The elevated accumulation of [^{18}F]-FEPPA induced by sevoflurane exposure was clearly attenuated by the coadministration of ALC, but since there were no or only a few significant differences to begin with, it was not possible to demonstrate a statistically significant effect of ALC here. No significant effects as compared to controls were detected in the animals exposed to ALC alone.

On PND 14, approximately 7 days after the anesthetic exposure, the uptake of [^{18}F]-FEPPA in the temporal area and thalamus was still higher in the sevoflurane-exposed animals than in the controls at most of the time points, but again these effects were not statistically significant (figs. 6B and 7B).

By PND 30, or about 21 days after anesthetic exposure, SUV values in the temporal lobe were not different between any of the experimental groups, whereas in the thalamus, they were still highest in the sevoflurane-exposed group, but not statistically significant compared to the controls. The values for the sevoflurane plus ALC group were indistinguishable from the control group (figs. 6C and 7C).

Consistent with observations for the frontal lobe, at the age of 2 and 6 months, the uptake of [^{18}F]-FEPPA in the temporal lobe and thalamus in anesthetic-exposed monkeys was similar to that of controls at most time points, and no significant differences were observed at any time (data not shown).

Discussion

Little information is available about the effects of developmental exposure to sevoflurane.[56,57] However, preclinical studies have demonstrated that early exposure to general anesthetics, such as ketamine, isoflurane, nitrous oxide, and

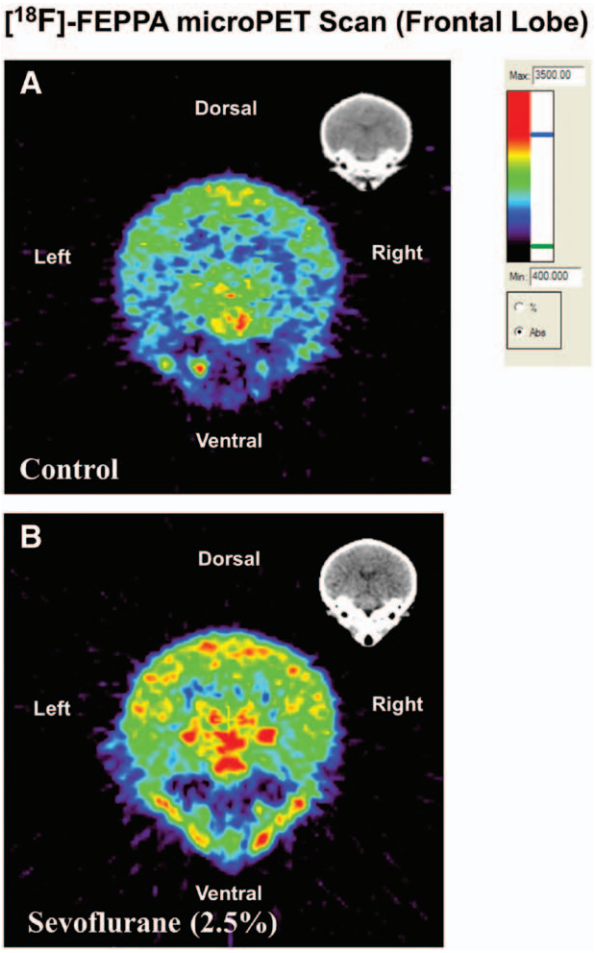

Fig. 3. A set of representative micro-positron emission tomography (microPET) images (coronal plane) of a control (*A*) and a treated monkey brain (*B*) 1 day after an 8-h exposure to 2.5% sevoflurane. (*A*, *B*) The appropriate computed tomographic images for anatomical registration. Compared with the control, the ^{18}F-labeled fluoroethoxybenzyl-*N*-(4-phenoxypyridin-3-yl) acetamide (^{18}F-FEPPA) signal uptake was significantly increased in the sevoflurane-exposed monkey infant in the frontal cortex. Color bar scales for images are given as 400 to 3500 nCi/cc.

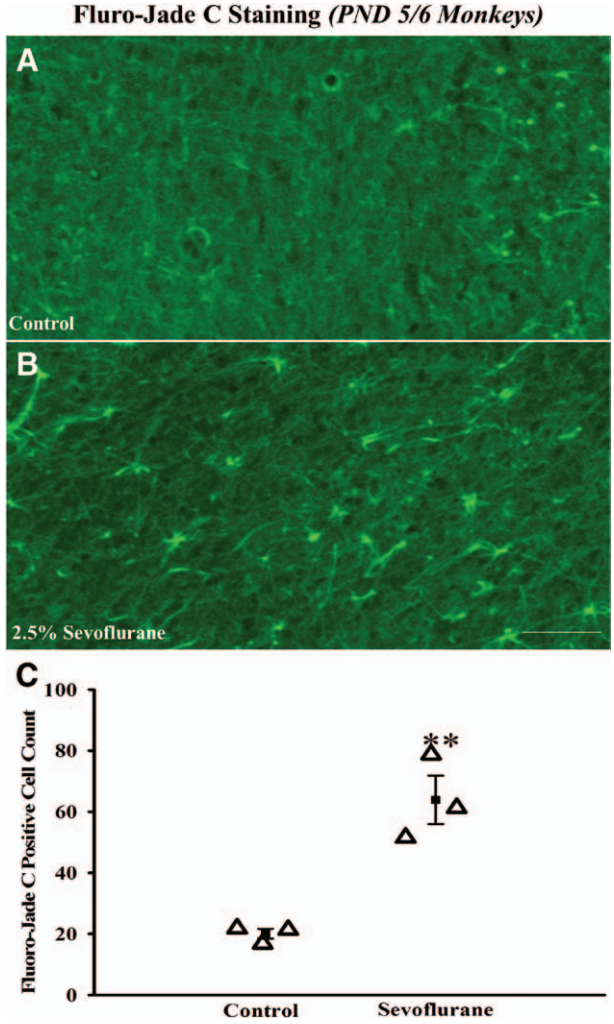

Fig. 4. Representative examples of Fluoro-Jade C staining of the frontal cortex of the developing monkey brain. Only a few Fluoro-Jade C–positive neuronal profiles were observed in a control monkey (*A*). Enhancement of neurotoxicity as evidenced by an increased number of Fluoro-Jade C–positive neuronal cells in sevoflurane-exposed monkey brain (*B*). Statistical analysis (*C*) indicates that sevoflurane (2.5%) exposure (8 h, n = 3/group) resulted in a significant increase in number of degenerative neurons in frontal cortex compared with controls (n = 3/group). *Scale bar* = 50 μm. $^{**}P < 0.01$. PND = postnatal day.

sevoflurane, induces widespread neuronal apoptosis in many brain regions in rodent models.[5,6,17,21,25,49,50,58,59] In a previous study,[60] we also provided evidence of sevoflurane-induced neurotoxicity and some observations on the temporal features of this effect in neonatal rats. The first report describing neuronal cell damage in nonhuman primates exposed perinatally to anesthetics was published in 2007.[50] Because the brain growth spurt in both human and nonhuman primates extends over a much longer time period than that observed in the rat, matching the timing of developmental events between humans and nonhuman primates is less problematic than matching the same between primates and rodents.[48,61,62]

In the current study, microPET/CT technology was employed to investigate whether a relatively long-term exposure (8 h) to clinically relevant doses of sevoflurane (2.5%) could induce toxic processes in the brain of the nonhuman primate and whether such effects could be attenuated by the antioxidant agent ALC. Our data demonstrated that an 8-h exposure of neonatal monkeys to sevoflurane at a clinically relevant concentration did not significantly disturb critical physiologic parameters compared with those of control, demonstrating that the sevoflurane-induced effect observed here was not attributed to compromised homeostatic mechanisms.

Recent studies have demonstrated that the up-regulation of TSPOs is related to numerous nervous system disorders, including neurotoxic brain damage.[45,63–66] In the CNS, the

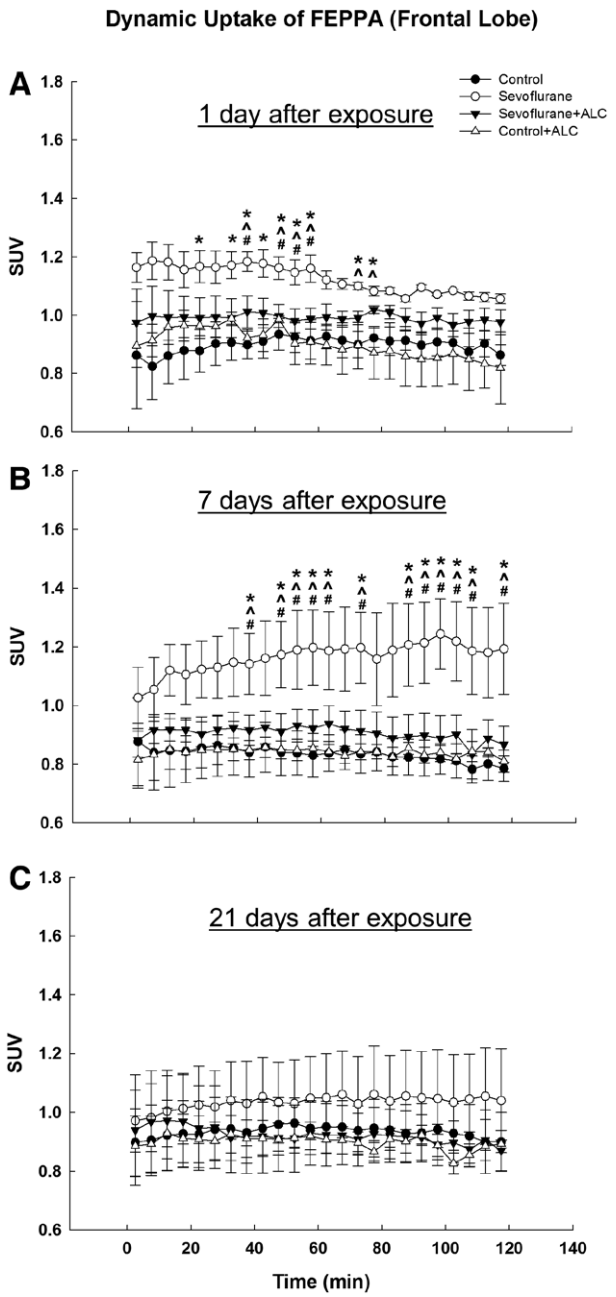

Fig. 5. Graph showing the dynamic uptake of ^{18}F-labeled fluoroethoxybenzyl-*N*-(4-phenoxypyridin-3-yl) acetamide (^{18}F-FEPPA) expressed as standard uptake value (SUV) *versus* time in a region of interest (ROI) in the left frontal cortex from control, sevoflurane-treated, sevoflurane + acetyl-L-carnitine (ALC), and control + ALC monkeys (n = 4/group) 1 day (*A*), 7 days (*B*), and 21 days after exposure (*C*). SUV = average concentration of radioactivity in the ROI (MBq/ml) × body weight in grams/injected dose (megabecquerel). Data are shown as the mean ± SEM. **P* < 0.05, sevoflurane *vs.* control; ^*P* < 0.05, sevoflurane *vs.* control + ALC; #*P* < 0.05, sevoflurane *vs.* sevoflurane + ALC.

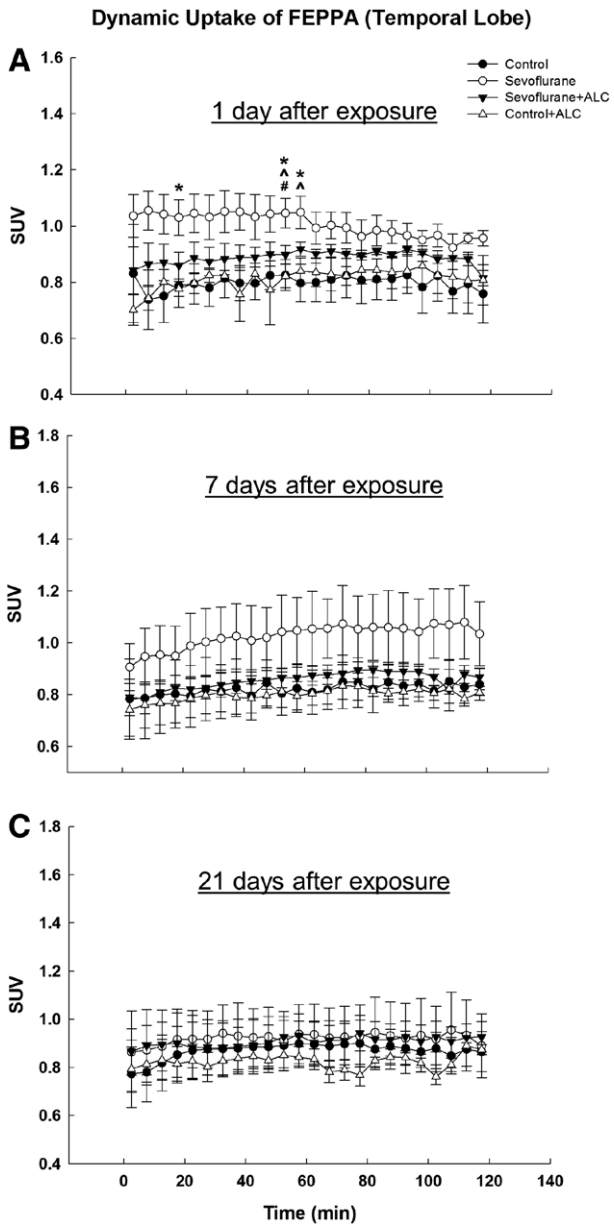

Fig. 6. Graph showing the dynamic uptake of ^{18}F-labeled fluoroethoxybenzyl-*N*-(4-phenoxypyridin-3-yl) acetamide (^{18}F-FEPPA) expressed as standard uptake value (SUV) *versus* time in a region of interest in the left temporal cortex from control, sevoflurane-treated, sevoflurane + acetyl-L-carnitine (ALC), and control + ALC monkeys (n = 4/group) 1 day (*A*), 7 days (*B*), and 21 days after exposure (*C*). Data are shown as the mean ± SEM. **P* < 0.05, sevoflurane *vs.* control; ^*P* < 0.05, sevoflurane *vs.* control + ALC; #*P* < 0.05, sevoflurane *vs.* sevoflurane + ALC.

up-regulated expression of TSPO has been regarded as a biomarker of activated microglia.[66–68] Such microglial activation usually begins within several hours after toxic insult and lasts for several days.[69–71] [^{18}F]-FEPPA is a specific TSPO ligand that can be efficiently synthesized at high radiochemical yields with high specific activity that has proven useful in nonhuman primate studies.[40,41,43,47,72–74] Due to the increased expression of TSPOs in areas of neuronal injury/neurotoxicity, [^{18}F]-FEPPA can be used as a marker for microglial activation and an indirect marker for neuronal damage, injury, and neurotoxicity. TSPO is recognized as an

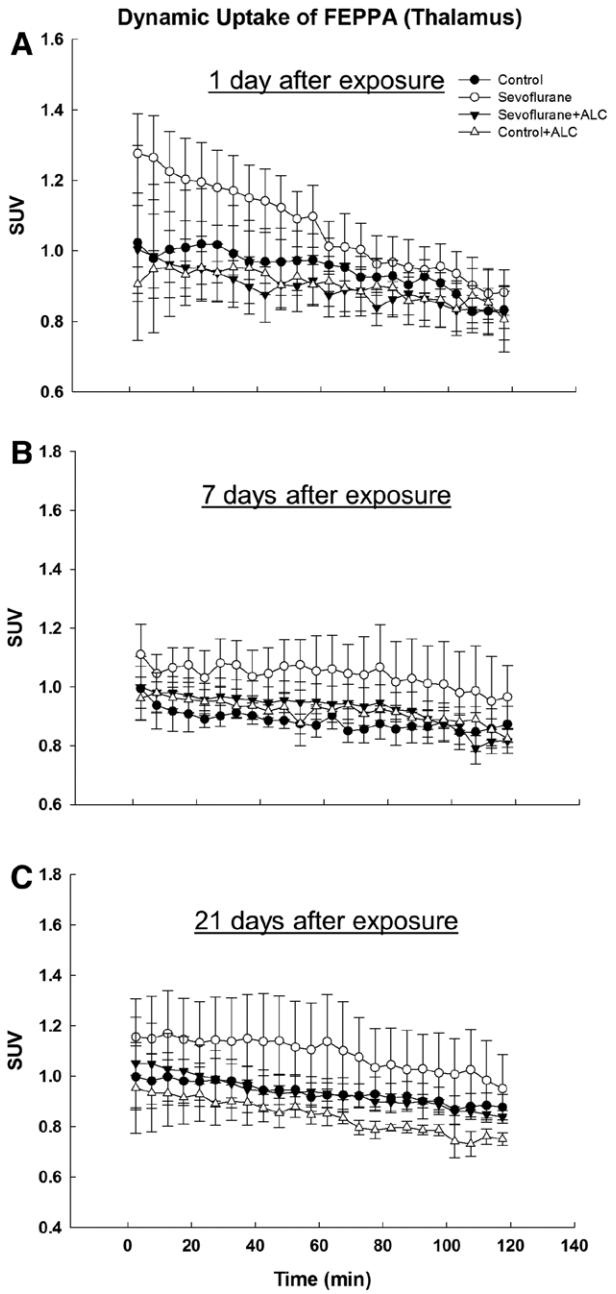

Fig. 7. Graph showing the dynamic uptake of ^{18}F-labeled fluoroethoxybenzyl-*N*-(4-phenoxypyridin-3-yl) acetamide (^{18}F-FEPPA) expressed as standard uptake value (SUV) *versus* time in a region of interest in the left thalamus from control, sevoflurane-treated, sevoflurane + acetyl-L-carnitine (ALC), and control + ALC monkeys (n = 4/group) 1 day (*A*), 7 days (*B*), and 21 days after exposure (*C*). Data are shown as the mean ± SEM.

important surrogate of associated neurotoxicity, which can be monitored using PET imaging using appropriate radioligands such as [^{18}F]-FEPPA.[40,41,43]

In the current study, [^{18}F]-FEPPA was used to repeatedly visualize and quantify, in the same animal, aspects of possible adverse neuronal effects associated with developmental exposure to sevoflurane. Increased accumulation of [^{18}F]-FEPPA was interpreted as increased levels of TSPO expression, representing neuroinflammation induced by neuronal insults, such as sevoflurane exposure.

Previous data from rodent models have demonstrated that sevoflurane can be toxic to the developing brain, and some studies have reported cognitive deficits in later life after such exposures.[23,27,28,75,76] However, definitive studies that clearly delineate the association between the pediatric use of general anesthetics and sedatives and developmental neurotoxicity are highly desired. In the current study, [^{18}F]-FEPPA was effectively taken up and concentrated into brain ROIs in both control and anesthetic-treated monkeys after intravenous injection. Signal levels of [^{18}F]-FEPPA, and presumably TSPO, were significantly elevated in multiple brain regions within 1 day after sevoflurane exposure, an effect that lasted for at least 1 week. This observation suggests increased microglial activation and astrocytosis in response to sevoflurane-induced neuronal effects. This effect seemed to last for about 3 weeks after exposure, at least in the frontal lobe and thalamus, as evidenced by increased retention of [^{18}F]-FEPPA, although by this time the effects were no longer statistically significant. These observations in the developing monkey are concordant with those observed in the developing rodent model.[60] On the other hand, sevoflurane-induced neural effects in the nonhuman primate were observed in multiple brain areas including the frontal cortex and temporal lobe and the thalamus, whereas in the rat, it was seen primarily in the frontal cortex. The current data indicate yet again that adverse effects associated with general anesthesia (in this case sevoflurane) are expressed in a time- and region-specific fashion. Although causality is presently unclear and probably multifactorial, the severity, as well as the pattern of gaseous anesthetic-induced neural damage, depends on the amount (dose) given, the duration of exposure, the route of administration, the receptor subtype activated, and the stage of development at the time of exposure. These factors are important because they can help identify thresholds of exposure for producing neurotoxicity in the developing nervous system. Toward this end, our high-resolution microPET/CT scanners, coupled with the appropriate radiotracer, have been able to provide *in vivo* molecular imaging at a sufficient resolution to resolve both major structures and neuronal activities in the nonhuman primate brain.

Consistent with the microPET/CT data, sevoflurane-induced neurotoxicity was confirmed and further characterized in the neonatal monkey brain by pathologic measurement. In this current study, Fluoro-Jade C staining was applied to confirm the presence of sevoflurane-induced neuronal damage at the cellular level. Fluoro-Jade C is a neuronal stain, which has a high affinity for degenerating neurons, regardless of specific insult or mechanism of cell death.[54] Pathologically, direct evidence of enhanced neuronal damage in the infant monkeys exposed to sevoflurane was obtained as indicated by increased numbers of Fluoro-Jade C–positive/neurodegenerative neurons in the frontal cortical area.

The pharmacologic blockade of excitatory NMDA receptors during development is thought to result in the subsequent up-regulation of NMDA receptors, resulting in a subsequent overexcitation from physiologic levels of glutamate.[50,77,78] The activation of GABA receptors during early development is actually excitatory, whereas in adults, this is inhibitory. Thus, inhibition of NMDA receptors or the stimulation of GABA receptors can increase overall excitability of the CNS and lead to excessive neuronal damage in the developing rodent and nonhuman primate. Studies have shown that sevoflurane activates glycine and GABA receptors while antagonizing NMDA receptors.[17–20,79] Although the underlying mechanisms are largely unknown, increased oxidative stress associated with mitochondrial dysfunction seems to play an important role in anesthetic-induced neurotoxicity.[28,80,81]

From our lipidomic analyses,[82] we noted that alterations in mitochondrial membrane morphology and function were particularly significant, suggesting that mitochondria may be the most vulnerable initial target of anesthesia-induced developmental neurotoxicity. To further explore potential mechanisms underlying anesthetic-induced neuronal damage and to evaluate possible protective strategies, ALC, an antioxidant and mitochondrial membrane–stabilizing agent involved in fatty acid transport and metabolism,[30,83–86] was coadministered with sevoflurane. ALC is an esterified form of LC that exists in relatively high levels in the brain.[86–89] In contrast to LC, ALC is more easily transported across the blood–brain barrier and, therefore, likely has a more rapid and perhaps a greater effect on brain metabolism.[90–93] ALC acts to preserve cellular membrane integrity and plays a critical role in mitochondrial oxidation of long-chain fatty acids. It is thought to provide neuroprotection in neurodegenerative diseases and situations of metabolic stress such as ischemia, hypoxia, aging, and alcoholism and in traumatic injury.[31–34,86,94–99] Thus, increased levels of ALC could enhance the capability of the mitochondrial antioxidant system and decrease the incidence of free radical-induced damage.

In our previous pediatric anesthetic study, mitochondrial viability was significantly attenuated in a dose-dependent manner after prolonged exposure to propofol, suggesting that the elevated mitochondrial production of reactive oxygen species is involved in producing anesthetic-induced cell damage.[100] In our previous studies,[39,40] neuronal damage was suggested in PND 14 rat pups that were exposed to different general anesthetics, including sevoflurane, on PND 7. The anesthetic-induced neuronal apoptosis observed in those studies was also attenuated by the coadministration of ALC. In the current study, coadministration of ALC did not affect the level of consciousness during sevoflurane-induced general anesthesia. Coadministration of ALC effectively attenuated the increased uptake of the TSPO tracer in multiple brain regions of developing nonhuman primates exposed to sevoflurane. These data strongly suggest that gaseous anesthetics can cause oxidative damage and dysfunction, likely *via* disruption of mitochondrial function that subsequently manifests as damage to neural cells.

In summary, it has been demonstrated that a single 8-h exposure to sevoflurane did not cause significant alterations in critical homeostatic mechanisms. MicroPET data indicate that exposing the developing monkey brain to sevoflurane during a period of rapid brain development can induce adverse effects in several brain regions including the frontal cortex, temporal lobe, and the thalamus, as evidenced by increases in microglial activation. Coadministration of ALC did not have any significant effect on depth of anesthesia, although it blocked, at least partially, the anesthetic-induced neuronal effects. The levels of TSPO in the CNS are thought to be important biomarkers of pathogenic processes, and the ability to track such levels using microPET technology provides a minimally invasive approach for investigating the location, time course, and severity of neurotoxic insults. The use of a nonhuman primate model combined with molecular imaging tools would seem to provide the most expeditious approach toward decreasing the uncertainty in extrapolating preclinical data to the human condition.

Research Support

This work was supported by the National Center for Toxicological Research, Jefferson, Arkansas, and the Center for Drug Evaluation and Research/U.S. Food and Drug Administration (FDA), Silver Spring, Maryland. This document has been reviewed in accordance with U.S. FDA policy and approved for publication. Approval does not signify that the contents necessarily reflect the position or opinions of the FDA nor does mention of trade names or commercial products constitute endorsement or recommendation for use. The findings and conclusions in this report are those of the authors and do not necessarily represent the views of the FDA.

Competing Interests

The authors declare no competing interests.

Correspondence

Address correspondence to Dr. Zhang: Division of Neurotoxicology, National Center for Toxicological Research/FDA, 3900 NCTR Road, Jefferson, Arkansas 72079. xuan.zhang@fda.hhs.gov. Information on purchasing reprints may be found at www.anesthesiology.org or on the masthead page at the beginning of this issue. Anesthesiology's articles are made freely accessible to all readers, for personal use only, 6 months from the cover date of the issue.

References

1. Bianchi SL, Tran T, Liu C, Lin S, Li Y, Keller JM, Eckenhoff RG, Eckenhoff MF: Brain and behavior changes in 12-month-old Tg2576 and nontransgenic mice exposed to anesthetics. Neurobiol Aging 2008; 29:1002–10
2. Xie Z, Dong Y, Maeda U, Moir RD, Xia W, Culley DJ, Crosby G, Tanzi RE: The inhalation anesthetic isoflurane induces a vicious cycle of apoptosis and amyloid beta-protein accumulation. J Neurosci 2007; 27:1247–54

3. Zhang X, Xue Z, Sun A: Subclinical concentration of sevoflurane potentiates neuronal apoptosis in the developing C57BL/6 mouse brain. Neurosci Lett 2008; 447:109–14
4. Zheng SQ, An LX, Cheng X, Wang YJ: Sevoflurane causes neuronal apoptosis and adaptability changes of neonatal rats. Acta Anaesthesiol Scand 2013; 57:1167–74
5. Ikonomidou C, Bosch F, Miksa M, Bittigau P, Vöckler J, Dikranian K, Tenkova TI, Stefovska V, Turski L, Olney JW: Blockade of NMDA receptors and apoptotic neurodegeneration in the developing brain. Science 1999; 283:70–4
6. Jevtovic-Todorovic V, Hartman RE, Izumi Y, Benshoff ND, Dikranian K, Zorumski CF, Olney JW, Wozniak DF: Early exposure to common anesthetic agents causes widespread neurodegeneration in the developing rat brain and persistent learning deficits. J Neurosci 2003; 23:876–82
7. Zhang X, Paule MG, Newport GD, Sadovova N, Berridge MS, Apana SM, Kabalka G, Miao W, Slikker W Jr, Wang C: MicroPET imaging of ketamine-induced neuronal apoptosis with radiolabeled DFNSH. J Neural Transm (Vienna) 2011; 118:203–11
8. Paule MG, Li M, Allen RR, Liu F, Zou X, Hotchkiss C, Hanig JP, Patterson TA, Slikker W Jr, Wang C: Ketamine anesthesia during the first week of life can cause long-lasting cognitive deficits in rhesus monkeys. Neurotoxicol Teratol 2011; 33:220–30
9. DiMaggio C, Sun LS, Kakavouli A, Byrne MW, Li G: A retrospective cohort study of the association of anesthesia and hernia repair surgery with behavioral and developmental disorders in young children. J Neurosurg Anesthesiol 2009; 21:286–91
10. Istaphanous GK, Loepke AW: General anesthetics and the developing brain. Curr Opin Anaesthesiol 2009; 22:368–73
11. Kalkman CJ, Peelen L, Moons KG, Veenhuizen M, Bruens M, Sinnema G, de Jong TP: Behavior and development in children and age at the time of first anesthetic exposure. Anesthesiology 2009; 110:805–12
12. Nie H, Peng Z, Lao N, Dong H, Xiong L: Effects of sevoflurane on self-renewal capacity and differentiation of cultured neural stem cells. Neurochem Res 2013; 38:1758–67
13. Wilder RT, Flick RP, Sprung J, Katusic SK, Barbaresi WJ, Mickelson C, Gleich SJ, Schroeder DR, Weaver AL, Warner DO: Early exposure to anesthesia and learning disabilities in a population-based birth cohort. Anesthesiology 2009; 110:796–804
14. Li Y, Liu C, Zhao Y, Hu K, Zhang J, Zeng M, Luo T, Jiang W, Wang H: Sevoflurane induces short-term changes in proteins in the cerebral cortices of developing rats. Acta Anaesthesiol Scand 2013; 57:380–90
15. Zhou X, Song FH, He W, Yang XY, Zhou ZB, Feng X, Zhou LH: Neonatal exposure to sevoflurane causes apoptosis and reduces nNOS protein expression in rat hippocampus. Mol Med Rep 2012; 6:543–6
16. Lerman J, Sikich N, Kleinman S, Yentis S: The pharmacology of sevoflurane in infants and children. Anesthesiology 1994; 80:814–24
17. Brosnan RJ, Thiesen R: Increased NMDA receptor inhibition at an increased sevoflurane MAC. BMC Anesthesiol 2012; 12:9
18. Hollmann MW, Liu HT, Hoenemann CW, Liu WH, Durieux ME: Modulation of NMDA receptor function by ketamine and magnesium. Part II: Interactions with volatile anesthetics. Anesth Analg 2001; 92:1182–91
19. Nishikawa K, Harrison NL: The actions of sevoflurane and desflurane on the gamma-aminobutyric acid receptor type A: Effects of TM2 mutations in the alpha and beta subunits. Anesthesiology 2003; 99:678–84
20. Tagawa T, Sakuraba S, Kimura K, Mizoguchi A: Sevoflurane in combination with propofol, not thiopental, induces a more robust neuroapoptosis than sevoflurane alone in the neonatal mouse brain. J Anesth 2014; 28:815–20
21. Fang F, Xue Z, Cang J: Sevoflurane exposure in 7-day-old rats affects neurogenesis, neurodegeneration and neurocognitive function. Neurosci Bull 2012; 28:499–508
22. Piehl E, Foley L, Barron M, D'Ardenne C, Guillod P, Wise-Faberowski L: The effect of sevoflurane on neuronal degeneration and GABAA subunit composition in a developing rat model of organotypic hippocampal slice cultures. J Neurosurg Anesthesiol 2010; 22:220–9
23. Satomoto M, Satoh Y, Terui K, Miyao H, Takishima K, Ito M, Imaki J: Neonatal exposure to sevoflurane induces abnormal social behaviors and deficits in fear conditioning in mice. Anesthesiology 2009; 110:628–37
24. Wang Y, Cheng Y, Liu G, Tian X, Tu X, Wang J: Chronic exposure of gestation rat to sevoflurane impairs offspring brain development. Neurol Sci 2012; 33:535–44
25. Liang G, Ward C, Peng J, Zhao Y, Huang B, Wei H: Isoflurane causes greater neurodegeneration than an equivalent exposure of sevoflurane in the developing brain of neonatal mice. Anesthesiology 2010; 112:1325–34
26. Lu Y, Wu X, Dong Y, Xu Z, Zhang Y, Xie Z: Anesthetic sevoflurane causes neurotoxicity differently in neonatal naïve and Alzheimer disease transgenic mice. Anesthesiology 2010; 112:1404–16
27. Takaenoki Y, Satoh Y, Araki Y, Kodama M, Yonamine R, Yufune S, Kazama T: Neonatal exposure to sevoflurane in mice causes deficits in maternal behavior later in adulthood. Anesthesiology 2014; 120:403–15
28. Yonamine R, Satoh Y, Kodama M, Araki Y, Kazama T: Coadministration of hydrogen gas as part of the carrier gas mixture suppresses neuronal apoptosis and subsequent behavioral deficits caused by neonatal exposure to sevoflurane in mice. Anesthesiology 2013; 118:105–13
29. Liu F, Patterson TA, Sadovova N, Zhang X, Liu S, Zou X, Hanig JP, Paule MG, Slikker W Jr, Wang C: Ketamine-induced neuronal damage and altered *N*-methyl-D-aspartate receptor function in rat primary forebrain culture. Toxicol Sci 2013; 131:548–57
30. Zou X, Sadovova N, Patterson TA, Divine RL, Hotchkiss CE, Ali SF, Hanig JP, Paule MG, Slikker W Jr, Wang C: The effects of L-carnitine on the combination of, inhalation anesthetic-induced developmental, neuronal apoptosis in the rat frontal cortex. Neuroscience 2008; 151:1053–65
31. Abdul HM, Butterfield DA: Involvement of PI3K/PKG/ERK1/2 signaling pathways in cortical neurons to trigger protection by cotreatment of acetyl-L-carnitine and alpha-lipoic acid against HNE-mediated oxidative stress and neurotoxicity: Implications for Alzheimer's disease. Free Radic Biol Med 2007; 42:371–84
32. Abdul HM, Calabrese V, Calvani M, Butterfield DA: Acetyl-L-carnitine-induced up-regulation of heat shock proteins protects cortical neurons against amyloid-beta peptide 1-42-mediated oxidative stress and neurotoxicity: Implications for Alzheimer's disease. J Neurosci Res 2006; 84:398–408
33. Ishii T, Shimpo Y, Matsuoka Y, Kinoshita K: Anti-apoptotic effect of acetyl-l-carnitine and I-carnitine in primary cultured neurons. Jpn J Pharmacol 2000; 83:119–24
34. Zanelli SA, Solenski NJ, Rosenthal RE, Fiskum G: Mechanisms of ischemic neuroprotection by acetyl-L-carnitine. Ann N Y Acad Sci 2005; 1053:153–61
35. Aliev G, Liu J, Shenk JC, Fischbach K, Pacheco GJ, Chen SG, Obrenovich ME, Ward WF, Richardson AG, Smith MA, Gasimov E, Perry G, Ames BN: Neuronal mitochondrial amelioration by feeding acetyl-L-carnitine and lipoic acid to aged rats. J Cell Mol Med 2009; 13:320–33
36. Hillmer AT, Wooten DW, Moirano JM, Slesarev M, Barnhart TE, Engle JW, Nickles RJ, Murali D, Schneider ML, Mukherjee J, Christian BT: Specific α4β2 nicotinic acetylcholine receptor binding of [F-18]nifene in the rhesus monkey. Synapse 2011; 65:1309–18

37. Kilbourn MR, Hockley B, Lee L, Sherman P, Quesada C, Frey KA, Koeppe RA: Positron emission tomography imaging of (2R,3R)-5-[(18)F]fluoroethoxybenzovesamicol in rat and monkey brain: A radioligand for the vesicular acetylcholine transporter. Nucl Med Biol 2009; 36:489–93
38. Wooten DW, Moraino JD, Hillmer AT, Engle JW, Dejesus OJ, Murali D, Barnhart TE, Nickles RJ, Davidson RJ, Schneider ML, Mukherjee J, Christian BT: *In vivo* kinetics of [F-18] MEFWAY: A comparison with [C-11]WAY100635 and [F-18] MPPF in the nonhuman primate. Synapse 2011; 65:592–600
39. Zhang X, Liu S, Paule MG, Newport GD, Callicott R, Berridge MS, Apana SM, Slikker WJ, Wang C: Protective effects of acetyl L-carnitine on inhalation anesthetic-induced neuronal damage in the nonhuman primate. J Mol Pharm Org Process Res 2013; 1:1–7
40. Zhang X, Newport GD, Paule MG, Liu S, Berridge MS, Apana SM, Ali SF, Slikker W Jr, Wang C: Quantitative assessment of acetyl-carnitine effects on anesthetic-induced neuronal death using MicroPET/CT imaging. J Drug Alcohol Res 2013:2
41. Zhang X, Paule MG, Newport GD, Liu F, Callicott R, Liu S, Berridge MS, Apana SM, Slikker W Jr, Wang C: MicroPET/CT imaging of [18F]-FEPPA in the nonhuman primate: a potential biomarker of pathogenic processes associated with anesthetic-induced neurotoxicity. ISRN Anesthesiol 2012:11
42. Zhang X, Paule MG, Newport GD, Zou X, Sadovova N, Berridge MS, Apana SM, Hanig JP, Slikker W Jr, Wang C: A minimally invasive, translational biomarker of ketamine-induced neuronal death in rats: MicroPET Imaging using 18F-annexin V. Toxicol Sci 2009; 111:355–61
43. Zhang X, Paule MG, Wang C, Slikker W Jr: Application of microPET imaging approaches in the study of pediatric anesthetic-induced neuronal toxicity. J Appl Toxicol 2013; 33:861–8
44. Imaizumi M, Briard E, Zoghbi SS, Gourley JP, Hong J, Fujimura Y, Pike VW, Innis RB, Fujita M: Brain and whole-body imaging in nonhuman primates of [11C]PBR28, a promising PET radioligand for peripheral benzodiazepine receptors. Neuroimage 2008; 39:1289–98
45. Lang S: The role of peripheral benzodiazepine receptors (PBRs) in CNS pathophysiology. Curr Med Chem 2002; 9:1411–5
46. Chen MK, Guilarte TR: Imaging the peripheral benzodiazepine receptor response in central nervous system demyelination and remyelination. Toxicol Sci 2006; 91:532–9
47. Wilson AA, Garcia A, Parkes J, McCormick P, Stephenson KA, Houle S, Vasdev N: Radiosynthesis and initial evaluation of [18F]-FEPPA for PET imaging of peripheral benzodiazepine receptors. Nucl Med Biol 2008; 35:305–14
48. Wang C: Advanced pre-clinical research approaches and models to studying pediatric anesthetic neurotoxicity. Front Neurol 2012; 3:142
49. Hotchkiss CE, Wang C, Slikker W Jr: Effect of prolonged ketamine exposure on cardiovascular physiology in pregnant and infant rhesus monkeys (*Macaca mulatta*). J Am Assoc Lab Anim Sci 2007; 46:21–8
50. Slikker W Jr, Zou X, Hotchkiss CE, Divine RL, Sadovova N, Twaddle NC, Doerge DR, Scallet AC, Patterson TA, Hanig JP, Paule MG, Wang C: Ketamine-induced neuronal cell death in the perinatal rhesus monkey. Toxicol Sci 2007; 98:145–58
51. Masimo Corporation: Masimo SEDLine™ System Operator's Manual. Irvine, Masimo Corporation, 2011
52. Prichep LS, Gugino LD, John ER, Chabot RJ, Howard B, Merkin H, Tom ML, Wolter S, Rausch L, Kox WJ: The Patient State Index as an indicator of the level of hypnosis under general anaesthesia. Br J Anaesth 2004; 92:393–9
53. Berridge MS, Apana SM, Hersh J: Teflon radiolysis as the major source of carrier in fluorine-18. J Label Compd Radiopharm 2009; 52:543–8
54. Schmued LC, Stowers CC, Scallet AC, Xu L: Fluoro-Jade C results in ultra high resolution and contrast labeling of degenerating neurons. Brain Res 2005; 1035:24–31
55. Zou X, Liu F, Zhang X, Patterson TA, Callicott R, Liu S, Hanig JP, Paule MG, Slikker W Jr, Wang C: Inhalation anesthetic-induced neuronal damage in the developing rhesus monkey. Neurotoxicol Teratol 2011; 33:592–7
56. Eger EI II: Characteristics of anesthetic agents used for induction and maintenance of general anesthesia. Am J Health Syst Pharm 2004; 61(suppl 4):S3–10
57. Myers R: The biological application of small animal PET imaging. Nucl Med Biol 2001; 28:585–93
58. Delgado-Herrera L, Ostroff RD, Rogers SA: Sevoflurance: Approaching the ideal inhalational anesthetic. A pharmacologic, pharmacoeconomic, and clinical review. CNS Drug Rev 2001; 7:48–120
59. Wang S, Peretich K, Zhao Y, Liang G, Meng Q, Wei H: Anesthesia-induced neurodegeneration in fetal rat brains. Pediatr Res 2009; 66:435–40
60. Liu S, Paule MG, Zhang X, Newport GD, Apana SM, Berridge MS, Patterson TA, Ali SF, Slikker W Jr, Wang C: The evaluation of sevoflurane-induced apoptotic neurodegeneration with microPET using [18F]-DFNSH in the developing rat brain. J Drug Alcohol Res 2013; 2:7
61. Dobbing J, Sands J: Comparative aspects of the brain growth spurt. Early Hum Dev 1979; 3:79–83
62. Workman AD, Charvet CJ, Clancy B, Darlington RB, Finlay BL: Modeling transformations of neurodevelopmental sequences across mammalian species. J Neurosci 2013; 33:7368–83
63. Benavides J, Fage D, Carter C, Scatton B: Peripheral type benzodiazepine binding sites are a sensitive indirect index of neuronal damage. Brain Res 1987; 421:167–72
64. Briard E, Zoghbi SS, Imaizumi M, Gourley JP, Shetty HU, Hong J, Cropley V, Fujita M, Innis RB, Pike VW: Synthesis and evaluation in monkey of two sensitive 11C-labeled aryloxyanilide ligands for imaging brain peripheral benzodiazepine receptors *in vivo*. J Med Chem 2008; 51:17–30
65. Oku N, Kashiwagi T, Hatazawa J: Nuclear neuroimaging in acute and subacute ischemic stroke. Ann Nucl Med 2010; 24:629–38
66. Papadopoulos V, Lecanu L, Brown RC, Han Z, Yao ZX: Peripheral-type benzodiazepine receptor in neurosteroid biosynthesis, neuropathology and neurological disorders. Neuroscience 2006; 138:749–56
67. Braestrup C, Albrechtsen R, Squires RF: High densities of benzodiazepine receptors in human cortical areas. Nature 1977; 269:702–4
68. Papadopoulos V, Baraldi M, Guilarte TR, Knudsen TB, Lacapère JJ, Lindemann P, Norenberg MD, Nutt D, Weizman A, Zhang MR, Gavish M: Translocator protein (18kDa): New nomenclature for the peripheral-type benzodiazepine receptor based on its structure and molecular function. Trends Pharmacol Sci 2006; 27:402–9
69. Banati RB: Neuropathological imaging: *In vivo* detection of glial activation as a measure of disease and adaptive change in the brain. Br Med Bull 2003; 65:121–31
70. Ito F, Toyama H, Kudo G, Suzuki H, Hatano K, Ichise M, Katada K, Ito K, Sawada M: Two activated stages of microglia and PET imaging of peripheral benzodiazepine receptors with [(11)C]PK11195 in rats. Ann Nucl Med 2010; 24:163–9
71. Takeuchi A, Isobe KI, Miyaishi O, Sawada M, Fan ZH, Nakashima I, Kiuchi K: Microglial NO induces delayed neuronal death following acute injury in the striatum. Eur J Neurosci 1998; 10:1613–20
72. Bennacef I, Salinas C, Horvath G, Gunn R, Bonasera T, Wilson AA, Laruelle M: Comparison of [11C]PBR28 and [18F]FEPPA as CNS peripheral benzodiazepine receptor PET ligands in the pig. J Nucl Med 2008; 49:81
73. Rusjan PM, Wilson AA, Bloomfield PM, Vitcu I, Meyer JH, Houle S, Mizrahi R: Quantitation of translocator protein binding in human brain with the novel radioligand [18F]-FEPPA and positron emission tomography. J Cereb Blood Flow Metab 2011; 31:1807–16

74. Schweitzer PJ, Fallon BA, Mann JJ, Kumar JS: PET tracers for the peripheral benzodiazepine receptor and uses thereof. Drug Discov Today 2010; 15:933–42
75. Dong Y, Zhang G, Zhang B, Moir RD, Xia W, Marcantonio ER, Culley DJ, Crosby G, Tanzi RE, Xie Z: The common inhalational anesthetic sevoflurane induces apoptosis and increases beta-amyloid protein levels. Arch Neurol 2009; 66:620–31
76. Shen X, Liu Y, Xu S, Zhao Q, Guo X, Shen R, Wang F: Early life exposure to sevoflurane impairs adulthood spatial memory in the rat. Neurotoxicology 2013; 39:45–56
77. Wang C, Sadovova N, Fu X, Schmued L, Scallet A, Hanig J, Slikker W: The role of the *N*-methyl-D-aspartate receptor in ketamine-induced apoptosis in rat forebrain culture. Neuroscience 2005; 132:967–77
78. Wang C, Sadovova N, Hotchkiss C, Fu X, Scallet AC, Patterson TA, Hanig J, Paule MG, Slikker W Jr: Blockade of *N*-methyl-D-aspartate receptors by ketamine produces loss of postnatal day 3 monkey frontal cortical neurons in culture. Toxicol Sci 2006; 91:192–201
79. Shelton KL: Discriminative stimulus effects of inhaled 1,1,1-trichloroethane in mice: Comparison to other hydrocarbon vapors and volatile anesthetics. Psychopharmacology (Berl) 2009; 203:431–40
80. Wang C, Zhang X, Liu F, Paule MG, Slikker W Jr: Anesthetic-induced oxidative stress and potential protection. Scientific World Journal 2010; 10:1473–82
81. Sanchez V, Feinstein SD, Lunardi N, Joksovic PM, Boscolo A, Todorovic SM, Jevtovic-Todorovic V: General anesthesia causes long-term impairment of mitochondrial morphogenesis and synaptic transmission in developing rat brain. Anesthesiology 2011; 115:992–1002
82. Liu F, Rainosek SW, Frisch-Daiello JL, Patterson TA, Paule MG, Slikker W Jr, Wang C, Han X: Potential adverse effects of prolonged sevoflurane exposure on developing monkey brain: From abnormal lipid metabolism to neuronal damage. Toxicol Sci 2015; 147:562–72
83. Arrigoni-Martelli E, Caso V: Carnitine protects mitochondria and removes toxic acyls from xenobiotics. Drugs Exp Clin Res 2001; 27:27–49
84. Patel SP, Sullivan PG, Lyttle TS, Rabchevsky AG: Acetyl-L-carnitine ameliorates mitochondrial dysfunction following contusion spinal cord injury. J Neurochem 2010; 114:291–301
85. Scafidi S, Racz J, Hazelton J, McKenna MC, Fiskum G: Neuroprotection by acetyl-L-carnitine after traumatic injury to the immature rat brain. Dev Neurosci 2010; 32:480–7
86. Virmani A, Binienda Z: Role of carnitine esters in brain neuropathology. Mol Aspects Med 2004; 25:533–49
87. Binienda Z, Virmani A, Przybyla-Zawislak B, Schmued L: Neuroprotective effect of L-carnitine in the 3-nitropropionic acid (3-NPA)-evoked neurotoxicity in rats. Neurosci Lett 2004; 367:264–7
88. Bresolin N, Freddo L, Vergani L, Angelini C: Carnitine, carnitine acyltransferases, and rat brain function. Exp Neurol 1982; 78:285–92
89. Shug AL, Schmidt MJ, Golden GT, Fariello RG: The distribution and role of carnitine in the mammalian brain. Life Sci 1982; 31:2869–74
90. Alves E, Binienda Z, Carvalho F, Alves CJ, Fernandes E, de Lourdes Bastos M, Tavares MA, Summavielle T: Acetyl-L-carnitine provides effective *in vivo* neuroprotection over 3,4-methylenedioximethamphetamine-induced mitochondrial neurotoxicity in the adolescent rat brain. Neuroscience 2009; 158:514–23
91. Calabrese V, Cornelius C, Mancuso C, Pennisi G, Calafato S, Bellia F, Bates TE, Giuffrida Stella AM, Schapira T, Dinkova Kostova AT, Rizzarelli E: Cellular stress response: A novel target for chemoprevention and nutritional neuroprotection in aging, neurodegenerative disorders and longevity. Neurochem Res 2008; 33:2444–71
92. Jones LL, McDonald DA, Borum PR: Acylcarnitines: Role in brain. Prog Lipid Res 2010; 49:61–75
93. McDaniel MA, Maier SF, Einstein GO: "Brain-specific" nutrients: A memory cure? Nutrition 2003; 19:957–75
94. Virmani A, Gaetani F, Binienda Z: Effects of metabolic modifiers such as carnitines, coenzyme Q10, and PUFAs against different forms of neurotoxic insults: Metabolic inhibitors, MPTP, and methamphetamine. Ann N Y Acad Sci 2005; 1053:183–91
95. Rump TJ, Abdul Muneer PM, Szlachetka AM, Lamb A, Haorei C, Alikunju S, Xiong H, Keblesh J, Liu J, Zimmerman MC, Jones J, Donohue TM Jr, Persidsky Y, Haorah J: Acetyl-L-carnitine protects neuronal function from alcohol-induced oxidative damage in the brain. Free Radic Biol Med 2010; 49:1494–504
96. Calabrese V, Giuffrida Stella AM, Calvani M, Butterfield DA: Acetylcarnitine and cellular stress response: Roles in nutritional redox homeostasis and regulation of longevity genes. J Nutr Biochem 2006; 17:73–88
97. Calabrese V, Ravagna A, Colombrita C, Scapagnini G, Guagliano E, Calvani M, Butterfield DA, Giuffrida Stella AM: Acetylcarnitine induces heme oxygenase in rat astrocytes and protects against oxidative stress: Involvement of the transcription factor Nrf2. J Neurosci Res 2005; 79:509–21
98. Virmani MA, Caso V, Spadoni A, Rossi S, Russo F, Gaetani F: The action of acetyl-L-carnitine on the neurotoxicity evoked by amyloid fragments and peroxide on primary rat cortical neurones. Ann N Y Acad Sci 2001; 939:162–78
99. Zaitone SA, Abo-Elmatty DM, Shaalan AA: Acetyl-L-carnitine and α-lipoic acid affect rotenone-induced damage in nigral dopaminergic neurons of rat brain, implication for Parkinson's disease therapy. Pharmacol Biochem Behav 2012; 100:347–60
100. Liu F, Rainosek SW, Sadovova N, Fogle CM, Patterson TA, Hanig JP, Paule MG, Slikker W Jr, Wang C: Protective effect of acetyl-L-carnitine on propofol-induced toxicity in embryonic neural stem cells. Neurotoxicology 2014; 42:49–57